European Review for Medical and Pharmacological Sciences 2019; 23 (3 Suppl): 294-303

Aldose reductase inhibitor Epalrestat alleviates high glucose-induced cardiomyocyte apoptosis *via* ROS

X. WANG[1], F. YU[2], W.-Q. ZHENG[3]

[1]Department of Pharmacy, Weihai Central Hospital, Weihai, China
[2]Department of Dermatology, Weihai Central Hospital, Weihai, China
[3]Department of Cardiology, Weihai Central Hospital, Weihai, China

Abstract. – OBJECTIVE: To clarify the role of aldose reductase inhibitor (ARI) in the high glucose-induced cardiomyocyte apoptosis and its mechanism.

MATERIALS AND MATHODS: In this study, H9c2 cardiomyocytes were employed as objects, high-glucose medium as stimulus, and ARI Epalrestat as a therapeutic drug. The cell apoptosis and activity changes of nitric oxide synthase (NOS), NO, and reactive oxygen species (ROS) were evaluated *via* Hoechst staining, enzyme-linked immunosorbent assay (ELISA), polymerase chain reaction (PCR), and Western blotting. In addition, the mitochondrial membrane potential was measured by fluorescence counting.

RESULTS: Epalrestat inhibited the activity of AR to improve high glucose induced oxidative stress in cardiomyocytes, weaken the activity, relieve the inhibition of activity, alleviate mitochondrial membrane potential damage, reduce the level of high glucose induced cardiomyocyte apoptosis, and suppress the expression and activity of caspase-3, thereby preventing high glucose induced cardiomyocyte apoptosis.

CONCLUSIONS: ARI protects against high glucose induced cardiomyocyte apoptosis.

Key words:
Aldose reductase inhibitor, High blood glucose, Apoptosis, ROS.

Introduction

With the aging of the population, as well as changes in people's lifestyle, the incidence rate of diabetes is increasing year by year in China, which has become a major public health issue. A survey revealed that over 70% of diabetic patients die of cardiovascular diseases and that the mortality is 2-4 times that of non-diabetic populations[1]. Therefore, diabetes-related cardiovascular complications are a leading cause of death in diabetic patients. Currently, scholars in China and elsewhere have considered diabetes as an independent risk factor for cardiovascular diseases[2]. High-glucose toxicity is the main factor damaging the heart and vessels, and the degree of such damage is closely correlated with the duration of hyperglycemia and level of blood glucose

Reports[3-5] have manifested that long-term high-glucose cannot only activate the renin-angiotensin-aldosterone system (RAAS), produce reactive oxygen species (ROS), and increase the advanced glycation end products (AGEs), as well as their receptors (RAGEs), but also activate inflammatory response and endoplasmic reticulum stress response, thereby promoting the damage and death of cardiomyocytes and vascular endothelial cells through various pathways. Hence, the current research hotspot is to explore the new mechanism of high glucose-induced damage to cardiomyocytes and vessels, and provide novel targets and measures for the prevention and treatment of diabetes-related cardiovascular complications.

The pathogenesis of diabetes is that glucose fails to be normally transformed into glycogen stores for a long time in the body of patients, thereby triggering the abnormally active reduction pathway of aldose. As a key enzyme in the polyol metabolism pathway, aldose reductase (AR) can reduce glucose into sorbitol which, with strong polarity, does not easily pass through cell membranes, but rather it accumulates in cells to alter the permeability of cells and weaken the

Corresponding Author: Wenqing Zheng, MM; e-mail: zhengwenqing369@163.com

Na^+-K^+-ATPase activity. This resulting in inositol loss and cell metabolism, as well as function impairment[6]. Since the drugs that block or attenuate AR activity can be used to prevent or delay the occurrence of diabetic complications, AR inhibitors (ARIs) have become therapeutic factors in the treatment of diabetes[7].

Thus, it was wondered whether high glucose-induced myocardial injury mechanism in diabetes involves aberrantly active aldose reduction pathways and whether ARIs are capable of improving high glucose-induced myocardial injury. Based on this hypothesis, this work aims to investigate the influence of ARIs on cardiomyocyte apoptosis and the regulatory mechanism of ROS therein, by establishing the high glucose-induced cardiomyocyte apoptosis model using ARIs and detecting AR activity, cell survival rate, ROS level, and changes in apoptosis-related indicators.

Materials and Methods

Culture of Cardiomyocytes

H9c2 cells were purchased from the Sha... Institute of Biochemistry and Cell Biolog... Chinese Academy of Sciences (Shanghai, C...). The cell suspension was transferred into a 1... centrifuge tube and added with 5 mL of Dulb... co's Modified Eagle Medium (...EM; Gibc... Rockville, MD, USA) contai... fetal bovine serum (FBS; Gibco, ...ville, ..., USA). After centrifugation at 1,... rpm for ... with the supernatant discarded, ...cel... with an appropriate v...me of ... containing 10% FBS, pipette... and mixed e... and their concentration w...usted to 1×... cells/mL. Next, the cells ...e ...ated into a 2... mL culture flask a...ultured ... incubator with 5% CO_2 at 37... and 24 h later, ...medium was replaced.

Ce...unti...Kit (CCK)-8 Assay

Th...e log...mic growth phase were ...sted, ...sted ... prepared into the suspension of the c...ion of 1×10^5cells/mL. Subseq...ly, they ...e seeded into a 96-well plate (10.../well). In the experiment, triplicate wells a... ...trols were set. After inoculation ...ernight, the cells were observed under a microscope to verify whether they adhered well. After t...t, each well of cells was cultured with 20 μL of MTT (3-(4,5-dimethylthiazol-2-yl)-2,5-diphenyl tetrazolium bromide; Sigma-Aldrich, St. Louis, MO, USA) at 37°C for 4 h. Next, with the supernatant sucked away carefully, each well of cells was added with 150 μL of dimethyl... (DMSO; Sigma-Aldrich, St. Louis, ... shaken, and mixed evenly. Final... the optical density (OD) of each well was ...ured at the wavelength of 570 nm using a mi... reader. The experiment was repeate... for thre... times.

Determination of L...te Dehydrogenase (...) Con...t

The cells in the log... ...ic ...wth ph... were digested, harves... and ...red in... suspension at th... ncentrati... ...cells/mL. Then, they ...eded into a ... plate (100 μL/well), ...e ...riment, tripl...ate wells and a control ...oup w... After cell attachment, the cu... plates were ...d in the incubator at 37... 5% CO_2 and c...red for 24 h. A total ... μL of the supernatant was obtained from ...h well, group... added with the corresponding ...ents accordi...o the kit instructions, mixed e... and let ...d at room temperature for 3 min..., a 1 cm light path cuvette was zeroed a... wavelength of 440 nm using double distilled water, and the OD was determined ...s of the microplate reader. The unit is ...in... as follows: 1,000 mL of culture solution reacts with matrices at 37°C for 15 min and 1 g/mol pyruvic acid produced in the reaction system is regarded as 1 unit. Finally, the content of LDH in the medium was calculated using the formula.

Hoechst Staining

All groups of cells cultured were inoculated into coverslips and treated in different groups, and once the supernatant was removed, they were washed using phosphate-buffered saline (PBS), fixed in Carnoy's solution and rinsed using PBS for 5 min. Then, the cells were stained with Hoechst 33258 working solution, let stand at room temperature for 15 min, rinsed with PBS again and sealed in the mixture of glycerin and PBS (1:1) or water-soluble mounting medium. Finally, the cells were observed under a fluorescence microscope. It was found that the cell nuclei displayed the blue fluorescence spots because the Hoechst stains are the specific fluorescence probe of deoxyribonucleic acid (DNA).

Polymerase Chain Reaction (PCR)

The cells treated were collected from each group to extract total ribonucleic acids (RNAs) using TRIzol (Invitrogen, Carlsbad, CA, USA).

After the concentration of samples was measured, RNAs were reversely transcribed into cDNAs in the first 40 cycles using the reverse transcription system according to the concentration. Then, PCR amplification was performed with the reverse transcription reaction conditions set. After each cycle, the fluorescence signals were collected in a real-time way, while the amplification and dissolution curves were plotted. Primer sequences used in this study were as follows: caspase 3, F: 5’-GTCCGGTACTCTCACTATACAC-3’, R: 5’-CGGTAAGGTTGTGTCACTTGGA-3’; NOS, F: 5’-GCCTGACACGGATACTACGGCAG-3’, R: 5’-GGATTACAGTCATGGCGCCAAG-3’; GAPDH: F: 5’- CGCTCTCTGCTCCTCCTGTTC -3’, R: 5’-ATCCGTTGACTCCGACCTTCAC-3’.

Detection of Caspase-3 Activity

After all groups of cells were collected, washed in PBS, and lysed with trypsin *via* an ice bath, the cell lysates were extracted to absorb cell medium for later use. Then, the adherent cells were digested using trypsin, transferred into the cell culture solution stored, mixed evenly with 2 mM Ac-DEVD-pNA, and incubated at 37°C for 60-120 [illegible]. The absorbance (A value) was measured [illegible] relatively obvious color changes were foun[illegible]

Western Blotting (WB)

The cells were taken from [illegible] group an[illegible] washed using D-Hank’s for [illegible]en, with the D-Hank’s blotted up u[illegible] absor[illegible]t paper, each group of cells was [illegible]ed with [illegible] of pre-cooled lysis buffer a[illegible]ed [illegible] min. Subsequently, [illegible] group [illegible]oteins were collected using a [illegible] scraper, p[illegible] in Eppendorf (EP) tube[illegible] centrifuged [illegible]C and 12,000 rpm. [illegible] su[illegible]tant was s[illegible]ked and transferred in[illegible] new E[illegible]es. After the protein con[illegible]ation was de[illegible]ned by the bicincho[illegible] acid (BCA) meth[illegible] (Pierce, Rockford, [illegible] USA)[illegible] proteins were mixed evenly wi[illegible] loa[illegible] buffe[illegible] and heated at 100°C for 6[illegible] total o[illegible] µL of proteins were [illegible]ded in [illegible] we[illegible]ith prepared separation [illegible]acer g[illegible]e electrophoresis was perfor[illegible] under a[illegible]per voltage in the buffer. After [illegible] with the gel clinging to polyvinylidene d[illegible]DF) membranes (Roche, Basel, [illegible]itzerland), the proteins were transferred on[illegible]e membranes in the transferring solution at 0[illegible] a constant voltage of 100 V for 60 min. After that, the PVDF membranes were sealed in 5% skim milk powder at room temperature for 1 h, while the protein bands were cut according to molecular weight and incubated with primary antibodies in a refrigerator at 4°C o[illegible]. On the second day, the PVDF mem[illegible] taken out, rinsed using Tris-B[illegible]ed Saline and Tween-20 (TBST), and inc[illegible]d with the secondary antibody IgG (1:5,000[illegible]om temperature for 1 h. After incu[illegible]tion, t[illegible]ducts were rinsed again using [illegible]T, followe[illegible] velopment and measur[illegible]nt of g[illegible]yscale [illegible] Tannon 5200 fluores[illegible] immu[illegible] development system.

Measureme[illegible]f Inhibi[illegible] Ra[illegible] AR

After bei[illegible]d in an ice [illegible]ells in each group we[illegible]ed at 4°C. [illegible]he colorless and tran[illegible]arent [illegible]atant was absorbed. Then [illegible]upernatan[illegible]dded into a 96-well pl[illegible] reaction wh[illegible] was initiated with t[illegible] addition of reductive coenzyme II (0.16 [illegible]ol/L) and D[illegible]lyceraldehyde substrate (10 [illegible]ol/L), while [illegible]A value at 340 nm was read c[illegible]uously u[illegible] the microplate reader within 40 [illegible]y of the inhibitory coenzyme metabo[illegible]ter the action of the enzyme and [illegible]ubstrate represented the activity of AR. Fi[illegible] inhibition curve was plotted with the [illegible]concentration as X-axis and inhibition rate as Y-axis.

Determination of ROS Concentration

The cells at the culture concentration of 6-8×10^4 cells/mL were taken from each group, sub-cultured in the medium for 24 h, and stimulated with stimuli at different concentrations for 8 h. After the culture solution was discarded, the cells were added with the intracellular total ROS probe CM-H2DCFDA at the final concentration of 5 pmol/L and incubated at 37°C in the dark for 30 min. After that, the probe was cleaned using PBS, the products were observed under a confocal laser scanning microscope at the excitation wavelength of 488 nm and an emission wavelength of 515 nm, and green fluorescence was seen. The screenshots of 8-10 cells were acquired in the field of view under a high-power microscope (600×). Finally, the fluorescence intensity was analyzed *via* software.

Determination of Nitric Oxide (NO) Concentration

The NO concentration was determined using the NO detection kit (Applygen Technologies, Beijing, China). After drug pretreatment or uric acid stimulation, the Roswell Park Memorial In-

stitute-1640 (RPMI-1640) medium was replaced with DMEM, and the supernatant of the cell medium was taken, centrifuged, and used for measurement of NO content. All the operations were performed strictly according to the methods in the kit instructions.

Detection of Mitochondrial Membrane Potential

The cells treated were collected and re-suspended in 0.5 mL of cell medium containing serum. Then, they were added with 0.5 mL of JC-1 staining working solution, bottomed up for several times, mixed evenly, and incubated in the incubator at 37°C in the dark for 30 min. The resulting cells were centrifuged at 600 g/min and 4°C, and once the supernatant was discarded, they were washed using 1× JC-1 staining buffer for 2 times, re-suspended in 1× JC-1 staining buffer, and centrifuged as above-mentioned for deposition. The supernatant was removed and the above washing step was repeated once. Finally, the fluorescence intensity was measured using a flow cytometer.

Statistical Analysis

Data were expressed as mean ± SD (s deviation) and the percentage of those in c ol group, and analyzed using Statistical Produc l Service Solutions (SPSS) 13.0 software (SI Inc., Chicago, IL, USA). The c risons b tween the two groups were m ndepen- dent samples *t*-test. Compa amo multiple groups was made using -way A fol- lowed by Post-Hoc Test (L ig ence). $p<0.05$ sugge that a difference was statistically si cant.

Results

Action Time Curve in High Glucose-Induced Cardiomyocyt

The cardiomyocytes were treated e DMEM medium containing 5.5, 22, 33, an mol/L glucose for 24, 48, and 72 h, respectiv a CCK-8 assay results showed that in t urviva f cardiomyocytes was lowered concentra time-dependent manner gure 1A and LD say results revealed t e sam d true for the degree of cardiomyoc m showi tatistically significant fere gure 1 <0.05). Moreover, aft eatment 3 l/L glucose for 48 l urvival rate iomyocytes reached (6 5. o 33 mmol/L nd 48 h were taken as t experi conditions.

Pr e Concentra of Epalrestat Cardiomyocytes Cultured in High cose

fter being ed using Epalrestat at the c trations 10 and 50 μmol/L for 48 h, the and injury degree of the cardiomyoc were detected *via* CCK-8 and LDH ssays, respectively. It was found that Epalrestat ignificant damage to cardiomyocytes at /L, and the difference was statistically significant (Figure 2, $p<0.05$). Subsequently, the experiment was conducted under the following conditions: Epalrestat at 1 and 10 μmol/L for 48 h.

Epalrestat Protected Cardiomyocytes from High Glucose-Induced Damage

According to the CCK-8 assay results, there was no statistical difference in the survival rate

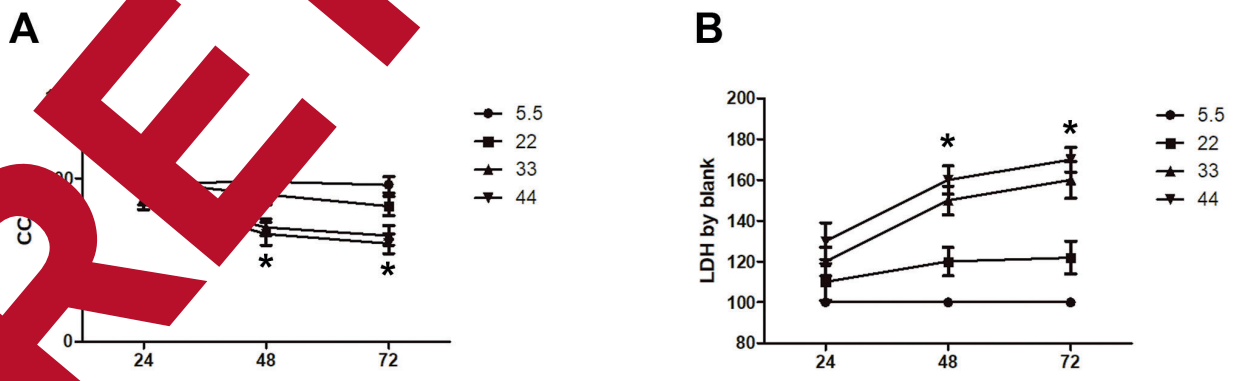

Fig . Effects of Glucose on Myocardial Cell Activity. *A,* CCK8 detects cell viability after 24h, 48h, and 72h of 5.5, 22, 33, 44 mmol/L glucose treatment. ***B,*** LDH detects cytotoxicity after 24h, 48h, and 72h of 5.5, 22, 33, 44 mmol/L glucose treatment. *compared with 5.5mmol/L glucose, $p< 0.05$.

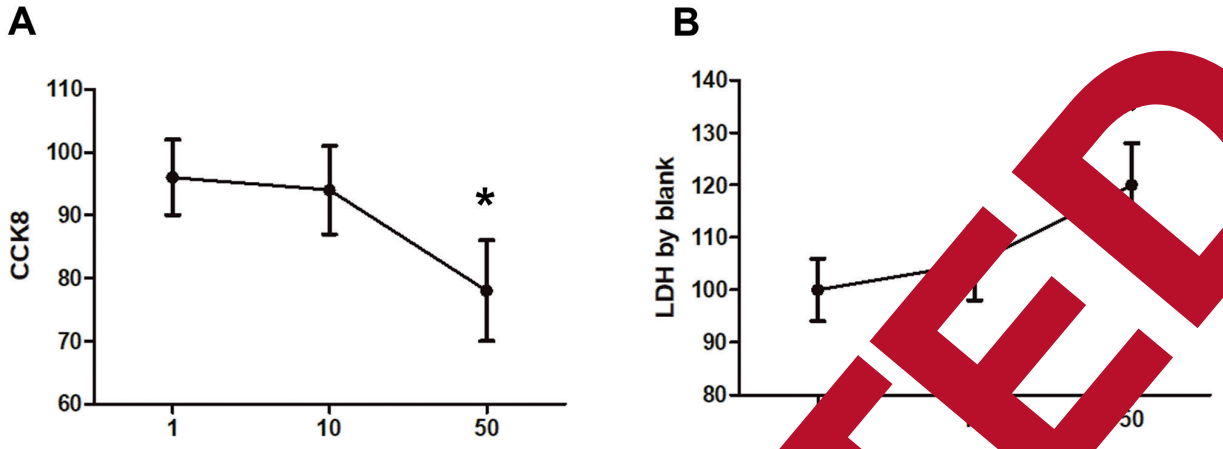

Figure 2. Effect of epalrestat on myocardial cell activity. ***A,*** CCK8 detects [illegible] after 48 h af[illegible] 10, 50 umol/L epalrestat treatment. ***B,*** LDH detects cytotoxicity after 48 h after 1, 10, 50 [illegible]/L ep[illegible] treatment. * compared with 1 umol/L epalrestat, $p<0.05$.

of cardiomyocytes between normal control group and mannitol group (Figure 3A, $p>0.05$, n=6), and compared with that in normal control group, the survival rate of cardiomyocytes was notably decreased in high glucose group, showing a statistically significant difference ($p<0.05$). In addition, no difference was found in the survival rate of cardiomyocytes between high glucose + 1 μmol/L Epalrestat group and high glucose group, while it was substantially raised in high glucose + 10 μmol/L Epalrestat group compared with that in high glucose group, showing a statistically significant difference ($p<0.05$). Similarly, the LDH activity results revealed that there was no statistical difference in the cardiomyocyte toxicity between normal control group and mannitol group (Figure [illegible], n=6), and compared with that in normal control group, the cardiomyocyte toxicity was notably increased in high glucose group, showing a statistically significant difference ($p<0.05$). Additionally, cardiomyocyte toxicity was not different between high glucose + 1 μmol/L Epalrestat group and high glucose group, while it was substantially raised in high glucose +

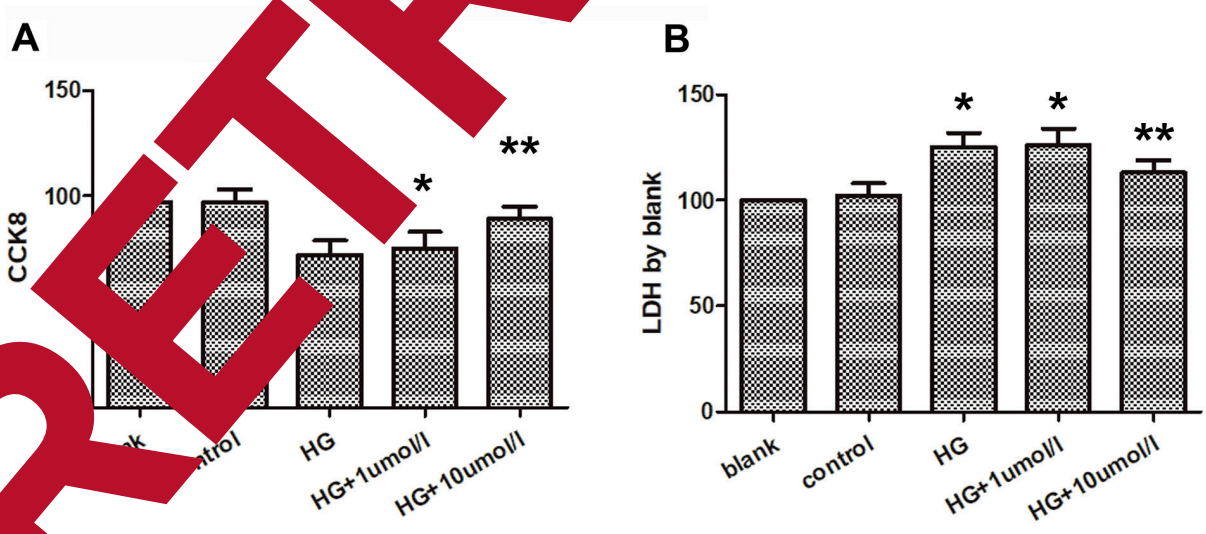

3. Epalrestat protects cultured cardiomyocytes from high glucose. ***A,*** CCK8 detects cell viability in blank, control, hig[illegible]ose group, 1 umol/L epalrestat treatment group, and 10 umol/l epalrestat treatment group. ***B,*** LDH detects cytotoxicity in blank, control, high glucose group, 1 umol/L epalrestat treatment group, and 10 umol/L epalrestat treatment group.* Compared with the blank group, $p<0.05$, ** compared with the high sugar group, $p<0.05$

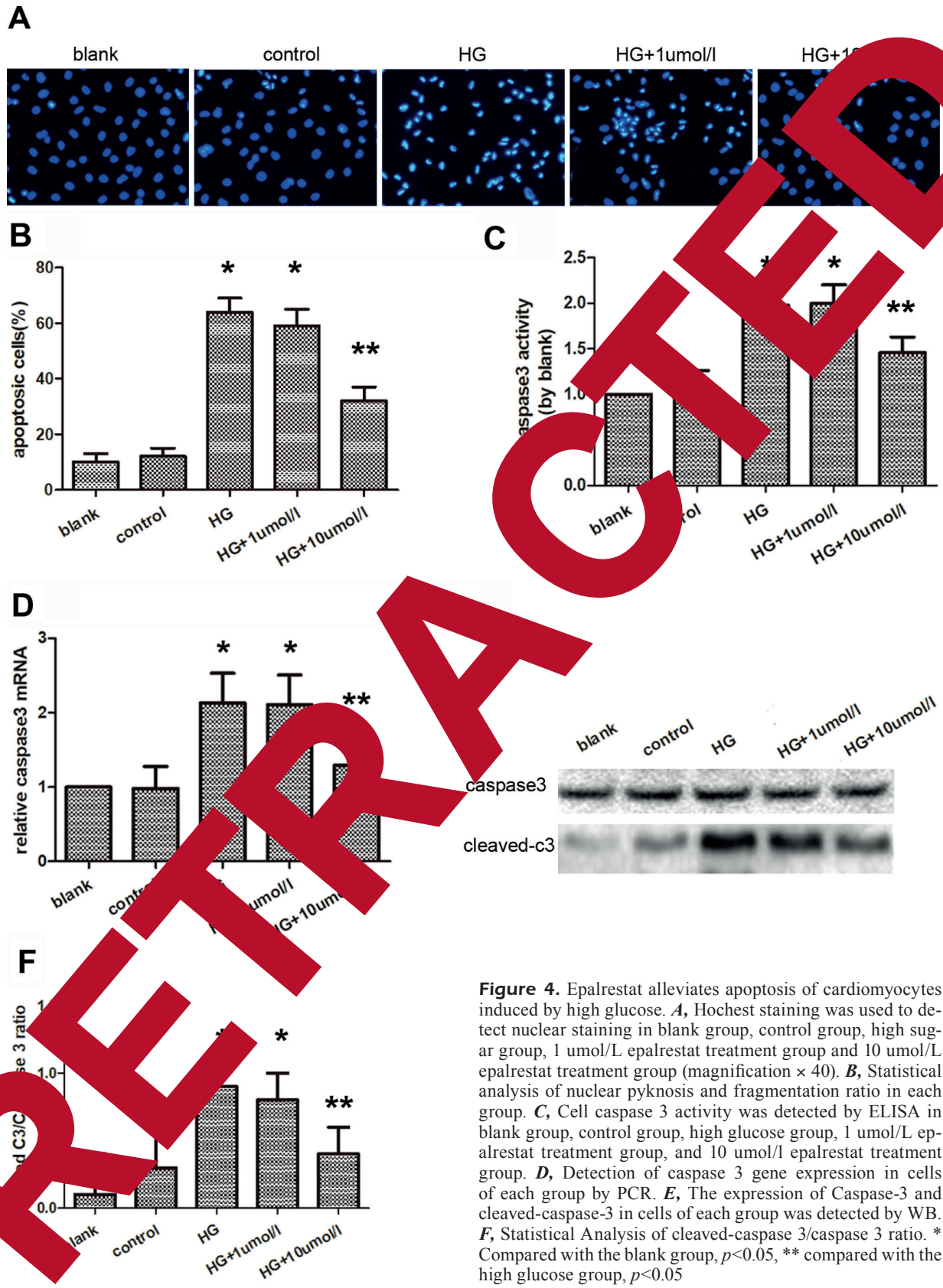

Figure 4. Epalrestat alleviates apoptosis of cardiomyocytes induced by high glucose. ***A,*** Hochest staining was used to detect nuclear staining in blank group, control group, high sugar group, 1 umol/L epalrestat treatment group and 10 umol/L epalrestat treatment group (magnification × 40). ***B,*** Statistical analysis of nuclear pyknosis and fragmentation ratio in each group. ***C,*** Cell caspase 3 activity was detected by ELISA in blank group, control group, high glucose group, 1 umol/L epalrestat treatment group, and 10 umol/l epalrestat treatment group. ***D,*** Detection of caspase 3 gene expression in cells of each group by PCR. ***E,*** The expression of Caspase-3 and cleaved-caspase-3 in cells of each group was detected by WB. ***F,*** Statistical Analysis of cleaved-caspase 3/caspase 3 ratio. * Compared with the blank group, $p<0.05$, ** compared with the high glucose group, $p<0.05$

10 μmol/L Epalrestat group compared with that in high glucose group, displaying a statistically significant difference ($p<0.05$).

Epalrestat Alleviated High Glucose-Induced Cardiomyocyte Apoptosis

Hoechst staining results revealed that compared with that in normal control group, the proportion of cells with karyopyknosis was evidently raised in high glucose group, displaying a statistically significant difference (Figure 4A, 4B, $p<0.05$, n=6). Moreover, it was not different between high glucose + 1 μmol/L Epalrestat group and high glucose group, but significantly decreased in high glucose + 10 μmol/L Epalrestat group compared with that in high glucose group. Also, $p<0.05$ was a statistically significant difference. PCR results indicated that high glucose group had a markedly higher gene expression level of Caspase-3 than normal control group, with a statistical difference (Figure 4C, $p<0.05$, n=6), and that it was evidently lowered in high glucose + 10 μmol/L Epalrestat group compared with that in high glucose group, also, $p<0.05$ was a statistically significance. It was found through enzyme-linked immunosorbent assay (ELISA) that the activity of Caspase-3 in high glucose group was significantly higher than that in normal control group, with a statistical difference (Figure 4D, $p<0.05$, n=6), and that it was evidently lowered in high glucose + 10 μmol/L Epalrestat group compared with that in high glucose group, showing a statistically significant difference ($p<0.05$). According to the WB results, the proportion of cleaved-Caspase-3 was significantly raised in high glucose group compared with that in normal control group, showing a statistical difference (Figure 4E, 4F, $p<0.05$, n=6), while the proportion was evidently lowered in high glucose + 10 μmol/L Epalrestat group compared with that in high glucose group, displaying a statistically significant difference ($p<0.05$).

Epalrestat Alleviated the Oxidative Stress in Cardiomyocytes

The detection results revealed that inhibition of AR was markedly decreased in high glucose group compared with that in normal control group (Figure 5A, $p<0.05$, n=6), and that there was no difference between high glucose + 1 μmol/L Epalrestat group and high glucose group, while it was evidently increased in high glucose + 10 μmol/L Epalrestat group compared with that in high glucose group ($p<0.05$). The NO synthase (NOS) gene expression was detected by PCR. It was discovered that the expression of NOS gene was markedly lowered in high glucose group compared with that in normal control group, showing a statistical difference (Figure 5B, $p<0.05$, n=6) and that it was evidently raised in high glucose + 10 μmol/L Epalrestat group compared with that in high glucose group ($p<0.05$). According to the determination results, the concentration of NO in high glucose group was significantly lower than that in normal control group (Figure 5C, $p<0.05$, n=6) and was evidently higher in high glucose + 10 μmol/L Epalrestat group than that in high glucose group ($p<0.05$). Additionally, high glucose group had a markedly higher level of ROS produced in cardiomyocytes than normal control group (Figure 5D, $p<0.05$, n=6), while the production level of ROS in cardiomyocytes was substantially reduced in high glucose + 10 μmol/L Epalrestat group compared with that in high glucose group, showing a statistically significant difference (Figure 5E, $p<0.05$, n=6). The JC-1 staining results manifested that the mitochondrial membrane potential was significantly decreased in high glucose group compared with that in normal control group ($p<0.05$), and it was higher in high glucose + 10 μmol/L Epalrestat group than that in high glucose group ($p<0.05$).

Discussion

A major cause of multiple diabetes-related complications is the abnormality of the polyol pathway directly induced by high glucose[8]. In recent years, the key enzymes in the polyol pathway, namely, AR and ARIs, have attracted much attraction[9]. With Epalrestat, an ARI widely applied in clinic, as the research object, the present study found that it exerted a protective effect against high glucose-induced cardiomyocyte injuries. Namely, it inhibited AR activity to attenuate oxidative stress and mitochondrial injury in cardiomyocytes, and reduce high glucose-induced cardiomyocyte apoptosis. Excessive activation of AR can result in circulatory disorders, and affect the activity of vascular endothelial and myocardial cells[5], thus weakening their reactivity to bioactive substances such as histamine and platelet-activating factor, aortas' reactivity to phenylephrine, and the relaxation

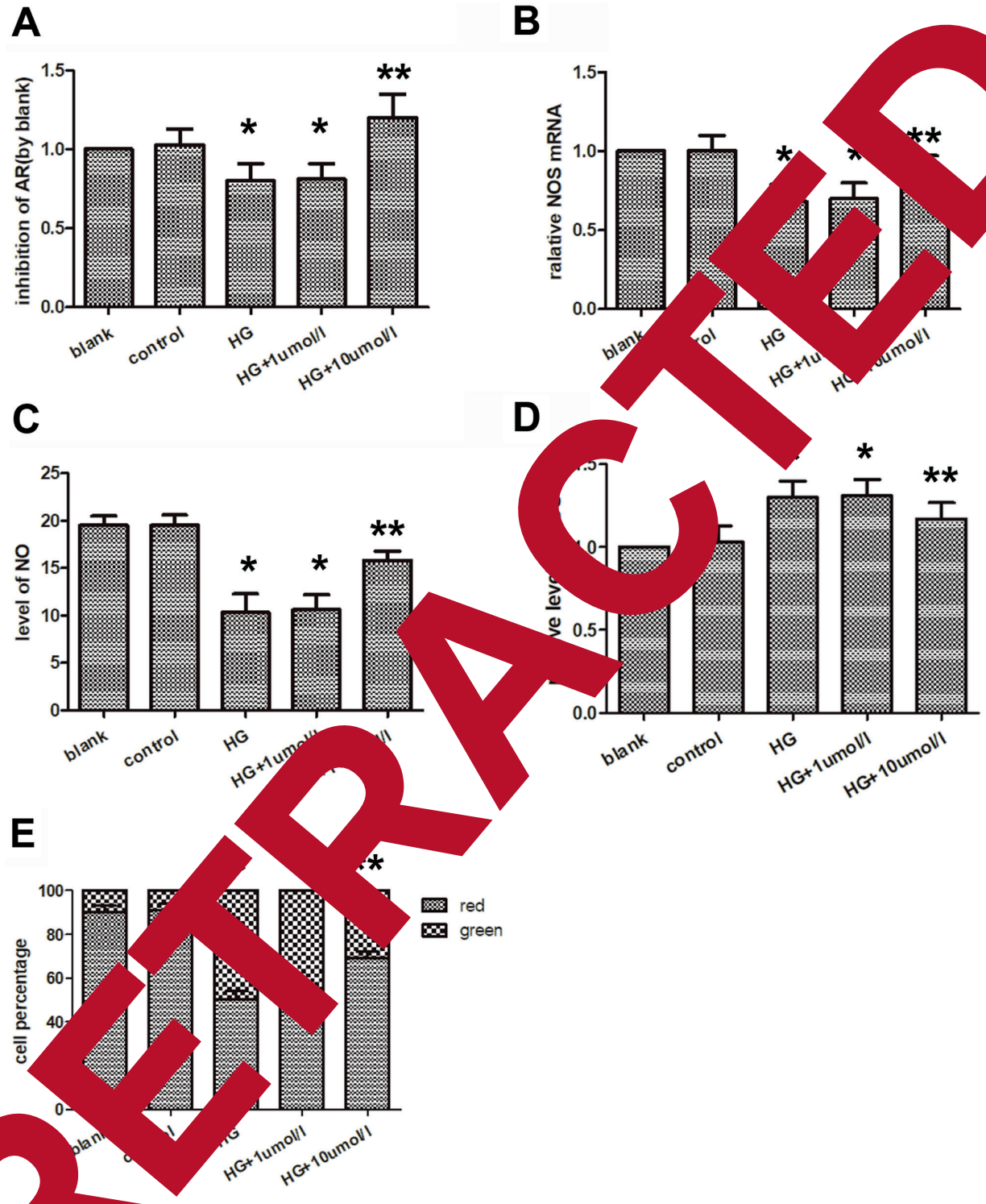

F[illegible]**stat ameliorates oxidative stress induced by high glucose in cardiomyocytes. *A,* Detection of Cell AR in-**[illegible]**ion was measured in blank group, control group, high sugar group, 1 umol/L epalrestat treatment group, and 10 umol/L **[illegible]**lrestat treatment group. *B,* Detection of NOS mRNA expression in cells of each group by PCR. *C,* Detection of NO Concen-**[illegible]**in Cells of Different Groups. *D,* Detection of ROS concentration in cells of each group. *E,* Detection of mitochondrial me**[illegible]**e potential changes in each group by JC-1. * Compared with the blank group, $p<0.05$, ** compared with the high gluco**[illegible]** group, $p<0.05$

of vascular endothelial cells by acetylcholine[4]. The intervention with ARIs can improve the microvascular reactivity to bradykinin, histamine, platelet-activating factor, and so on, significantly enhance the maximal contractile response of aortas to phenylephrine action, and restore acetylcholine-dependent vasodilation in endothelium[10,11]. The above effects may be realized through NOS.

It has been found in clinical research that Epalrestat, non-competitive ARIs, is capable of relieving diabetic peripheral neuropathy, autonomic neuropathy, fundus disease, and renal lesions[11-13]. Also, there were few findings in the study of diabetic cardiomyopathy: the diabetic patients with neuropathy and decreased cardiac ejection fraction were randomly divided into ARI treatment group and placebo group. The 1-year follow-up results showed that the left ventricular ejection fraction, cardiac output, and left ventricular stroke volume under resting conditions, as well as left ventricular ejection fraction in motion state, were notably improved in ARI treatment group. The efficacy was independent of blood pressure, insulin use, and abnormal heart rate vari... under baseline conditions, while the card... put, stroke volume, and end-diastolic volum... re all lowered in placebo group[14]. The above re... indicate that ARIs repress and even partially ... verse the worsening of diabetic c... function.

In this research, the hig... induced cardiomyocyte injury mo... was c... ructed, and it was discovered t... palres... viet-ed high glucose-induc... ati... inhibition on NO, ...uced ... production, and protected t... itochond... membrane potential from ... under oxi... stress, ultimately w... mi... activation of the intracellular apoptosis p... y, decreasing the proportio... apoptotic ce... d relieving high glucos... uced myocardial ... totoxicity. This expl... why E... restat can improve the disea... ditio... n diab... ic patients with cardiac ins... y to s... extent and provides a ...retic... is fo... treatment in those with ...ic car... thy.

Conclusions

...found that Epalrestat inhibited AR activity to a...viate oxidative stress, thereby improving high glucose-induced cardiomyocyte injuries.

Conflict of Interests

The Authors declare that they have no conflict of i...ts.

References

1) Hong XY, Lin J, Gu WW. Ri... factors ... rapies in vascular diseases: an ...rella revie... ed systematic reviews ... meta-analyses. Physiol 2019; 234: 8... 8232.
2) Yuan T, Yang T, C... Fu D..., Wang J, Yuan Q, Yu H, Xu W, Xie ... nits into ...lative stress and i... ma... ng diab... mellitus-acceler... atheros... Re... iol 2019; 20: 247-2...
3) Huynh ... o BC, McMu... K, Ritchie RH. Diab... ard... athy: mechanisms and new treatm... t strate... rgeting antioxidant signaling pathways. Pha... Ther 2014; 142: 375-...
...olpe C, Villar-Delfino PH, Dos AP, Nogueira-Machado JA. Cellula... death, reactive oxygen species (ROS) and d... ic complications. Cell Death Dis 2018; 9: 119.
...ang Z, Ho... Q, Zhang X, Xiao W, Wang L, Cui ... Z... Cai G, Chen X, Wu D. Aldose re... ates endothelial cell dysfunction induced by high uric acid concentrations. Cell Commun Signal 2017; 15: 3.
...M, Hemshekhar M, Kemparaju K, Girish KS. Ber... e mitigates high glucose-potentiated platelet aggregation and apoptosis by modulating aldose reductase and NADPH oxidase activity. Free Radic Biol Med 2019; 130: 196-205.
7) Huang Q, Liu Q, Ouyang D. Sorbinil, an aldose reductase inhibitor, in fighting against diabetic complications. Med Chem 2019; 15: 3-7.
8) Jin QS, Huang LJ, Zhao TT, Yao XY, Lin LY, Teng YQ, Kim SH, Nam MS, Zhang LY, Jin YJ. HOXA11-AS regulates diabetic arteriosclerosis-related inflammation via PI3K/AKT pathway. Eur Rev Med Pharmacol Sci 2018; 22: 6912-6921.
9) Soltesova Prnova M, Svik K, Bezek S, Kovacikova L, Karasu C, Stefek M. 3-Mercapto-5H-1,2,4-triazino[5,6-b]indole-5-acetic acid (Cemtirestat) alleviatessymptoms of peripheral diabetic neuropathy in Zucker diabetic fatty (ZDF) rats: arole of aldose reductase. Neurochem Res 2019; 44: 1056-1064.
10) Alam F, Shafique Z, Amjad ST, Bin AM. Enzymes inhibitors from natural sources with antidiabetic activity: a review. Phytother Res 2019; 33: 41-54.
11) Senthilkumari S, Sharmila R, Chidambaranathan G, Vanniarajan A. Epalrestat, an aldose reductase inhibitor prevents glucose-induced toxicity in human retinal pigment epithelial cells in vitro. J Ocul Pharmacol Ther 2017; 33: 34-41.
12) He J, Gao HX, Yang N, Zhu XD, Sun RB, Xie Y, Zeng CH, Zhang JW, Wang JK, Ding F, Aa JY, Wang GJ. The aldose reductase inhibitor epalrestat exerts nephritic protection on diabetic nephropathy in db/db mice through metabolic modulation. Acta Pharmacol Sin 2019; 40: 86-97.

13) Hotta N, Kawamori R, Fukuda M, Shigeta Y; Aldose Reductase Inhibitor-Diabetes Complications Trial Study Group. Long-term clinical effects of epalrestat, an aldose reductase inhibitor, on progression of diabetic neuropathy and other microvascular complications: multivariate epidemiological analysis based on patient background factors and severity of diabetic neuropathy. Diabet Med 2012; 29: 1529-1533.
14) Hu X, Li S, Yang G, Liu H, Boden G, Li L. Efficacy and safety of aldose reductase inhibitor treatment of diabetic cardiovascular autonomic neuropathy: systematic review and meta-analysis. PLoS One 2014; 9: e87096.